Significant Bandwidth Enhancement of Radial-Line Slot Array Antennas Using A Radially Non-Uniform TEM Waveguide

Mst Nishat Yasmin Koli, *Student Member, IEEE*, Muhammad U. Afzal, *Senior Member, IEEE*, and Karu P. Esselle, *Fellow, IEEE*

***Abstract*—Radial line slot array (RLSA) antennas have attractive features such as high gain, high efficiency, and planar low profile, but their gain bandwidths have been limited to less than 10%. This paper presents a method to significantly increase the gain bandwidth of RLSAs to over 30%. The key to the method is the application of a non-uniform radial TEM waveguide as opposed to the radially uniform TEM waveguide used in conventional RLSAs. Hence, the condition for maximum radiation is satisfied at a wide range of frequencies by different sections of the RLSA. To demonstrate the concept, several circularly polarised RLSA designs and one prototype are presented. The measured results of the prototype demonstrate an unprecedented 3dB gain bandwidth of 27.6%, a peak gain of 27.3 dBic, 3dB axial ratio bandwidth greater than 31.1% and a 10dB return loss bandwidth greater than 34.8%. The overall measured bandwidth of the RLSA in which gain variation and axial ratio are within 3dB and return loss is greater than 10dB is from 9.7 GHz to 12.8 GHz or 27.6%. Its extremely high measured gain bandwidth product per unit area (GBP/A) of 88 indicates excellent overall performance in terms of bandwidth, gain and area.**

***Index Terms*—Bandwidth improvement, circularly polarised, Gain Bandwidth Product, GBP, Gain Bandwidth Product per unit area, GBP/A, high gain, radial line, slot array, SATCOM, space, satellite, SOTM, wide band, wireless communication, 5G**

I. Introduction

MODERN wireless communication systems require wideband, low-profile, efficient and highly directive antennas. Designing a wideband antenna is often accompanied by compromises of gain, cost, size, or efficiency. Furthermore, some wireless systems, particularly for on-the-move-connectivity, use circular polarization (CP) to avoid loss due to polarization mismatch. A recently developed antenna beam-steering method for such mobile systems, now known as Near-Field Meta-Steering [1], [2] requires a low-profile, high-gain antenna with a fixed beam as the base antenna. With such a base antenna with sufficient bandwidth, this method can provide efficient beam steering over a wide bandwidth [3].

Radial line slot arrays (RLSAs) have the advantages of low profile, structural simplicity, high gains and high efficiencies [4]–[7]. In a typical RLSA, a radial waveguide is formed between two parallel metal sheets to support an outward propagating cylindrical TEM wave, and it's excited by a feeding probe at the center. A large array of radiating slots is strategically cut in the top plate to control the polarization and radiation pattern. The height of the waveguide is less than half of the guided wavelength to prevent the propagation of any higher-order modes. In the early 1960s, Goebels and Kelly [8] were first to demonstrate the use of a planar radial waveguide with annular slots for X-band applications. Later, in the 1980s, the RLSA antennas were investigated as a planar substitute to the well-known parabolic reflectors [4], [5], [9] in Japan, for direct broadcast satellite services at 12 GHz. An antenna with curved reflectors generally suffers from degradation of performances due to rain and snow build-up. Also, the large physical volume of reflector antennas makes them undesirable for this on-the-move wireless systems. When high antenna gains are required at high frequencies, in comparison with the well-known microstrip patch arrays, the RLSA antennas offer higher radiation efficiency [4], [6], [10], [11]. This is because RLSAs have very low conductor and dielectric losses mainly because, unlike a phased array, an RLSA does not have a feed distribution network.

RLSAs can be designed to radiate linear polarization (LP) or circular polarization (CP). This is be achieved by different strategic placements and orientations of the slots on the upper plate. Two different configurations of RLSA antennas have been investigated: single-layered and double-layered [4], [7], [11]–[22]. In a single-layered RLSA, slots are excited by a radially outward traveling transverse electromagnetic (TEM) wave, while in a double-layered RLAS they are excited by an inward traveling TEM wave [11], [23]–[28]. A single-layered RLSA is easier to manufacture but a double-layered RLSA can be designed to have a higher aperture efficiency [4], [6], [7], [11], [13], [26], [29].

One of the main limitations of the RLSAs is their narrow gain bandwidth[1] [4], [11]–[14], [19], [23], [26], [28], [30]–[34]. This is due to the design requirement of placing slots at a radial spacing of one guided wavelength to constructively create beam in the broadside direction. At any other frequency, the spacing between slots is either greater or less than the guided wavelength and the condition for maximum broadside radiation is not fulfilled. The bandwidth of an RLSA decreases with the

Mst Nishat Yasmin Koli is with the Centre for Collaboration in Electromagnetics and Antenna Engineering, School of Engineering, Macquarie University, Sydney, NSW 2109, Australia (e-mail: mst-nishat-yasmin.koli@students.mq.edu.au). Muhammad U. Afzal and Karu P. Esselle are with the School of Electrical and Data Engineering, University of Technology, Sydney, NSW 2007, Australia (e-mail: muhammad.afzal@uts.edu.au, karu.esselle@uts.edu.au).

[1]Gain bandwidth is the frequency range in which the gain remains within 3-dB of the maximum value.

increase of the aperture diameter due to the long line effect of travelling wave excitation feed [30], [35], [36]. To extend the bandwidth of RLSA, a structure of a radial waveguide was proposed with a hybrid of single-layered and double-layered RLSA [10], [30], [35], [37]. The feed structure consisted of two feed regions and a power divider and feed line length was shortened to half to increase the bandwidth. A high gain of 33.7 dBi was achieved with a 3-dB gain bandwidth of 6.7%. Another method was proposed to improve antenna efficiency and frequency bandwidth using matching termination slots [36]. Slots are arranged concentrically to reduce aperture blocking above the power divider. To improve the impedance bandwidth of RLSAs, many investigations have been conducted [38]–[43]. Utilization of low-cost FR4 materials, open-ended air gap, multilayered and square cavity and multi-sleeve coaxial transition are some of them.

In this paper, a new method is presented to substantially increase the gain bandwidth of RLSAs and the method is validated by designs and experimental results of RLSAs with up to 14,822% gain bandwidths. The key to this is making the waveguide radially nonuniform such that the condition for maximum broadside radiation is satisfied over a much larger frequency range than otherwise possible. The area of the antenna is much smaller than previous RLSAs with similar gains and in fact the gain bandwidth product per unit area of the antenna has reached unprecedented levels for an RLSA. Predicted and measured results confirm that antennas designed using this method have not only high gain but also good axial ratio and input matching over a wide bandwidth.

The paper is arranged such that the operating principle of the new antenna is explained in Section II, followed by its design method in Section III. Design examples are presented in Section IV. Full-wave simulated and measured results are given in Section V to validate the concept.

II. Principle of Operation

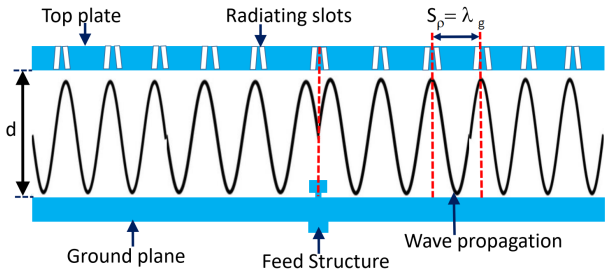

Fig. 1: Wave propagation in the uniform TEM radial waveguide of a conventional RLSA antenna. Note the same guided wavelength λ_g throughout, which, at design frequency, is equal to slot spacing S_ρ.

In order to understand the wideband operation of the new antenna, first it is important to understand how a conventional RLSA with a uniform TEM waveguide operates. The wave propagation in the radially uniform TEM waveguide of a conventional RLSA is illustrated in Fig. 1. As shown with more details in Fig. 2, this radial waveguide comprises two parallel circular metal plates, with the feeding probe at the center. The top metal plate has rings of radiating slots (Fig. 2(a))

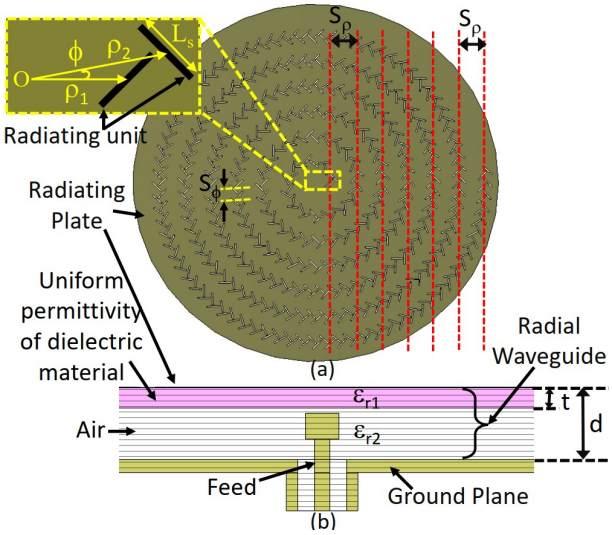

Fig. 2: (a) Top view: Slot arrangement on the top plate in a spiral pattern with radial separation S_ρ between adjacent slot rings, (b) Cross section of the radial waveguide.

while the bottom plate is the ground plane. The metal plates of the waveguide are separated by a distance d. The radial TEM waveguide is often partially filled with dielectric material as shown in Fig. 2. The purpose of the dielectric material is to slow the wave so that the guided wavelength (λ_g) is smaller than the free-space wavelength ($\lambda_\circ$) in order to avoid grating lobes in the radiation pattern. The effective dielectric constant of the TEM waveguide is the weighted sum of the dielectric constants of the dielectric material and air. In conventional RLSAs, the effective dielectric constant and hence the guided wavelength is uniform throughout the waveguide.

In CP-RLSAs, radiating slots on the top metal plate are arranged in pairs of two, as shown in Fig. 2. The two slots in a pair are orthogonal and thus radiate two orthogonal electric-field components with equal magnitudes [4], [20], [29]. Furthermore, the difference in radial distances of the two slot centres is set to a quarter of the guided wavelength (i.e. $\rho_2 - \rho_1 = \lambda_g/4$) to create a phase difference of 90°. The slots pair are arranged in a spiral to ensure constructive interference in the broadside direction [4], [20]. The direction of the spiral is anticlockwise in the right-hand CP RLSAs and clockwise in the left-hand CP RLSAs [4], [20]. The spacing between adjacent slot pairs in the radial direction and the spiral direction is denoted by S_ρ and S_ϕ, respectively. S_ϕ can be set arbitrarily based on slot density on the antenna aperture while S_ρ is made equal to the guide wavelength λ_g at the design frequency in order to produce constructive interference, and thus a beam of radiation in the broadside direction. At any other frequency, λ_g is different, and the condition for maximum broadside radiation i.e. $S_\rho = \lambda_g$ is not satisfied. Hence, conventional RLSAs with uniform radial waveguides are inherently narrowband.

The RLSA aperture field amplitude distribution is controlled by the lengths of radiating slots. In the TEM waveguide, the strength of the outward travelling mode reduces as it propagates from the center towards the edge. Additionally, the available power in TEM waveguide mode at the edge is less than that at

the center due to the radiation from the slot pairs in between. To mitigate the effects of too strong tapering of the outward travelling TEM mode, and hence to improve the amplitude distribution, the slot length (Ls) is increased as a function of radial distance [20] according to:

$$L_s = \delta + (\rho \times \alpha) \tag{1}$$

Where ρ is the radial distance of the slot center from the center of the aperture, δ is a constant factor that depends on the operating frequency, and α is the coupling coefficient that controls aperture amplitude taper. The product $(\rho \times \alpha)$ in this equation is referred to as the coupling factor. The coupling factor increases with the radial distance, which leads to larger slots. By varying the slot lengths this way, we control the proportion of energy coupled from the inner cavity field to the radiating field. A more detailed description of the slot design strategy that has also been followed in the proposed wideband RLSA is given in [20].

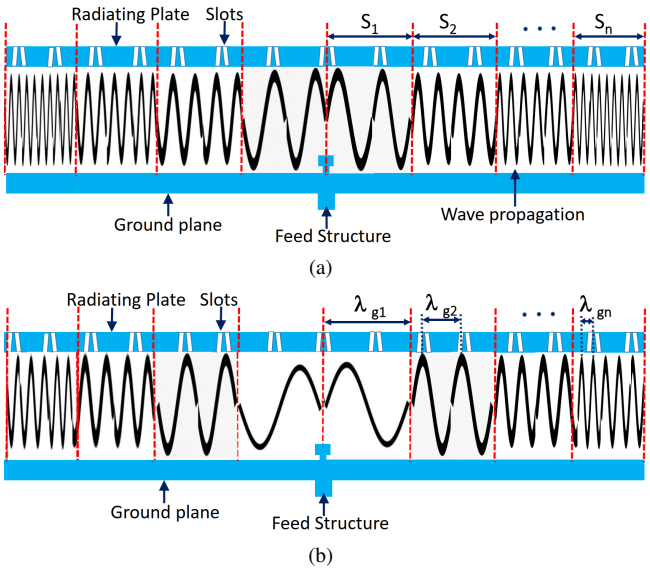

Fig. 3: (a) Outward wave propagation in a radially non-uniform TEM waveguide at frequency f_1. At this frequency, the first section S_1 satisfies the condition for maximum radiation. (b) Wave propagation in the same non-uniform TEM waveguide at a different frequency f_2. At this frequency, the second section S_2 satisfies the condition for maximum radiation.

To increase the bandwidth, we make the waveguide of the RLSA non-uniform radially. It can be gradually non-uniform but for the ease of fabrication in the examples presented in this paper, it is non-uniform stepwise, i.e. effective dielectric constant and guided wavelength changes in steps. Outward propagation of the wave in such a non-uniform radial waveguide is illustrated in Fig. 3. It passes through several sections (S_1, S_2 etc.) having different guided wavelengths.

Note that S_ρ is fixed throughout the antenna aperture to maintain the spiral slot layout of a conventional RLSA. The sections are designed such that at one frequency f_1, one section (S_1) satisfies the condition of maximum radiation, i.e. $S_\rho = \lambda_{g1}(f_1)$, and at another one frequency f_2, another section (S_2) satisfies the condition of maximum radiation, i.e. $S_\rho = \lambda_{g2}(f_2)$. Hence, this condition is at least approximately satisfied over a much larger range of frequencies using as many sections as required, resulting in an RLSA with much wider gain bandwidth.

In this design, we have kept slot spacing fixed on the aperture for the sake of simplicity, to prove the concept of bandwidth enhancement with minimal advanced slot refinements. More sophisticated slot (length and spacing) optimizations methods, including slot fine-tuning by taking into account the guided wavelength perturbation due to slot coupling to the parallel plate waveguide, have been developed in the past [4], [6], [10], [22], [34], and their application to this type of broadband RLSA has the potential to improve performance further.

It is to be mentioned here that, alternatively, slot positions can be varied in different sections while keeping guided wavelength constant in the waveguide. The advantage of changing guided wavelengths in different sections of the radial waveguide, however, is a simpler generation of slot layout in the model, which is done as in the case of conventional narrowband RLSAs. Hence, it was selected here to prove the concept of satisfying the maximum radiation condition in a wide range of frequencies using different sections of the RLSA.

III. Design Method

To design a wideband RLSA with the principle of operation outlined in the pervious section, we first break the required operating bandwidth of the antenna into several sub-bands (SB_1, SB_2 etc.). The first section S_1 is designed such that S_ρ is equal to λ_{g1} of that section at the centre frequency of the first sub-band. The effective dielectric constant (and actual dielectric constant of the dielectric layer) of this section are determined so. The next section S_2 is then designed such that the same condition is satisfied at the centre frequency of the next sub-band SB_2, and this is repeated to cover the required bandwidth.

To validate the concept, a CP-RLSA operating over a frequency range from 9 GHz to 13 GHz was designed. The slot layout was created following the design process discussed in the previous section and also reported for the uniform-waveguide-based RLSA reported in [20]. The slot layout (lengths and spacing) was generated at the centre operating frequency of 11 GHz and for a uniform TEM waveguide filled with a reference dielectric constant ϵ_r = 1.41. Hence a slot ring spacing (S_ρ = λ_g) of 22.73 mm was chosen for our RLSA design.

The target frequency band was broken into five 1 GHz sub-bands, each with the centre frequency listed in Table I. We require five different guided sections (S_1, S_2, S_3, S_4 and S_5) in the waveguide as shown in Fig. 4. Each section has a radial length of W_n (where n = 1, 2, ...5) and an equivalent relative permittivity of ϵ_r. At the centre of the antenna, the value of ϵ_r is the lowest and it increases towards the edge. The lengths (W_n) of sections may or may not be equal. The total radius R of the antenna aperture is equal to the radius of the top radiating plate.

Table I lists the calculated design parameters of the non-uniform waveguide such that the guided wavelength (λ_g) in

TABLE I: Non-uniform waveguide design parameters.

Centre frequency of the sub-band (f)	Free-space Wavelength (λ_{on})	Fixed Radial separation ($S_\rho = \lambda_{gn}$)	Radial separation in terms of λ_{on}	Required effective dielectric constant to radiate broadside at this frequency (ϵ_r)	Section
GHz	mm	mm	$\frac{S_\rho}{\lambda_{on}}$	$(\frac{\lambda_{on}}{S_\rho})^2$	S_n
9	33.3 (λ_{o1})	22.73	0 .68	2.15	S_5
10	30 (λ_{o2})	22.73	0.75	1.74	S_4
11	27.2 (λ_{o3})	22.73	0.83	1.43	S_3
12	25 (λ_{o4})	22.73	0.9	1.2	S_2
13	23.07 (λ_{o5})	22.73	0.98	1.03	S_1

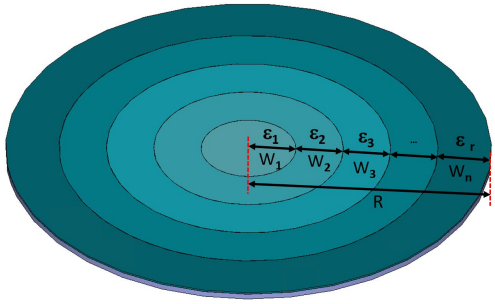

(a)

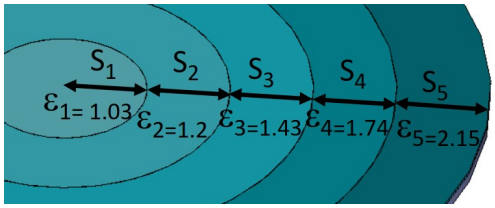

(b)

Fig. 4: Non-uniform radial waveguide configuration with five discrete sections.

each section at the centre frequency of the corresponding sub-band is equal to the fixed radial spacing (S_ρ) of slot rings, to obtain maximum radiation along z axis at this frequency. For example, at 9 GHz for a pre-defined radial spacing or S_ρ of 22.73 mm, one TEM waveguide section (S_5) must have an effective relative permittivity of $\epsilon_r = (\frac{\lambda_{oN}}{S_\rho})^2$ = 2.15. The calculated effective relative permittivity of each of the five sections of the non-uniform waveguide are given in the fifth column of Table I.

IV. Design Examples

A. Choice of Sectioning

In order to compare the performance of the new RLSAs with non-uniform waveguides with traditional RLSAs with radially uniform TEM waveguides, we designed a few of each type. Three conventional RLSAs have the same aperture and top radiating slot configuration but three different uniform radial waveguides with effective dielectric constants of 1.0, 2.2, and 3.0. Fig. 5 compares the broadside directivities of two non-uniform RLSAs with 5 and 10 sections with the directivities of the three conventional uniform RLSAs mentioned above. All results in Fig. 5 were predicted with full-wave simulations of different CP RLSAs. They were carried out using the Transient Solver in CST Microwave Studio. These RLSAs have the same slot layout, which is generated at 11 GHz and for a reference dielectric constant (ϵ_r) of 1.41.

The dielectric sections are annular or circular in shape and the slot pattern is a spiral, so dielectric boundaries falling between slot "rings" or even under some slots are unavoidable. In this analysis, we assumed continuous aperture field with the phase delay changing in accordance with the variation of the effective dielectric constant in each section. For slot layout design simplicity, we used the same slot spacing everywhere, which was calculated as for a conventional narrowband RLSA operating at a reference frequency of 11 GHz and with a constant effective dielectric constant of 1.41. In the design process, we have not made any changes to the slots that would fall on the boundary of the dielectrics and have kept the slot layout the same as otherwise. The overall effects of such slots are included in the full-wave simulations and they do not appear to making a noticeable overall performance. The lengths of these slots can be fine-tuned in future designs. All other design parameters such as the radius (R) of the top plate and the waveguide and the height of the waveguide (d) are the same as before. It can be seen from Fig. 5 that the two non-uniform RLSAs have much larger bandwidths than the conventional uniform RLSAs. The 3-dB directivity bandwidth of the RLSA with 10 sections is 4.8 GHz (7.8-12.6 GHz) whereas the bandwidths of the uniform RLSAs are in the range of 600 - 800 MHz. This increase in bandwidth comes at the expense of reduced peak directivity and aperture efficiency.

Although a large number of sections (N) increases the bandwidth, there is a compromise between bandwidth and peak directivity. Thus, like in many other antennas, as the directivity bandwidth increases, aperture efficiency drops. To further quantify this compromise, Table II compares the performance of six RLSAs with different number of sections (N) in terms of 3-dB directivity bandwidth, peak directivity and aperture efficiency. Note that the estimates of aperture efficiency shown in this table are for comparison purpose only as they were calculated assuming that the antenna is lossless and hence the gain is equal to directivity. All RLSAs have a radius of 200 mm. The effective permittivity of each section was determined following the procedure explained in the previous section. It can be seen that for N = 10, the 3-dB directivity bandwidth of 47% is possible with a peak directivity of 25.4 dBic. With decreasing number of sections, the bandwidth gradually decreases and the peak directivity increases. The uniform RLSAs (N = 1) have the best peak directivity and aperture efficiency but their 3-dB directivity bandwidths are less than 8%. Compared with very large and very small number of sections, N = 3 provides a good compromise between the directivity, 3-dB directivity bandwidth and structural complexity.

To study the effect of the permittivity values for a fixed number of sections (N), we have designed two different CP-RLSAs with the same value of N = 3 and those results are also listed in Table II. The reader may note that it is at the discretion of the antenna designer to keep the reference frequency (11

GHz) at the centre of a frequency band by keeping reference ϵ_r = 1.41 as an intermediate among dielectrics used for sections in the waveguide. As an example, in the first three sections RLSA design (3rd row in Table II), the three dielectric sections have dielectric constants of 1.03, 1.2, and 1.43. In the second design (4th row in Table II), the three dielectric sections have dielectric constants of 1.2, 1.43 and 1.74. In the former, the initial radial separation matches to the highest dielectric constant and the antenna has a peak directivity of 27.9 dBic while in the latter it is matched to an intermediate dielectric constant and the antenna has a higher peak directivity of 29.1 dBic. Thus, the design where slot spacing is matched to the intermediate dielectric constant has better directivity and aperture efficiency. Yet, the relationship to bandwidth is more complicated. Both designs have about the same operating bandwidth of 2 GHz but due to the upward shift of the bandwidth, the former has a larger percentage of 3-dB directivity bandwidth.

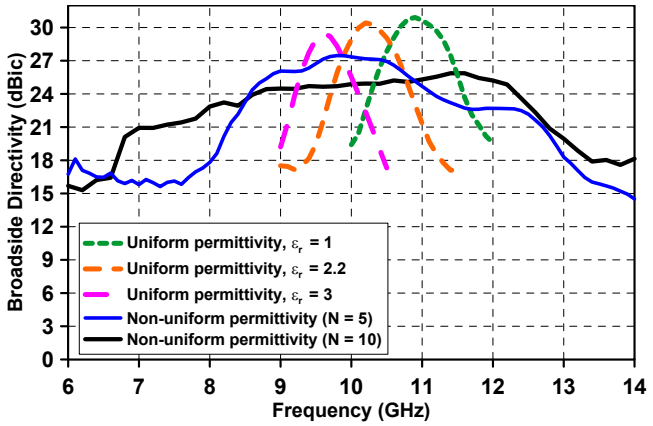

Fig. 5: Comparison of the broadside directivity of RLSAs with uniform and non-uniform multi-section radial waveguides.

TABLE II: Performance of RLSAs with different number of sections (N) in the radial waveguide.

Number of Sections	Length of each section	Effective permittivity	Frequency range	Peak directivity	3-dB directivity bandwidth	Aperture Efficiency
(N)	mm	$\{\epsilon_1, \epsilon_2, ...\epsilon_r\}$	GHz	(dBic)	(%)	(%)
10	20	0.68, 0.77, 0.88, 1.03, 1.2, 1.43, 1.74, 2.15, 2.72, 3.55	7 - 16	25.4	47	14
5	40	1.03, 1.2, 1.43, 1.74, 2.15	9 - 13	27.5	24.5	32
3	66.7	1.03, 1.2, 1.43	11 - 13	27.9	17.8	36.6
3	66.7	1.2, 1.43, 1.74	10 - 12	29.1	14	46
1	200	1.74	10	29.5	6.2	52.5
1	200	1.43	11	30.4	7.8	57

Another consideration is the length of each section in a multi-section non-uniform RLSA. In previous design all sections had the same length but they can be different. Table III summarises the performance of five tri-section (N = 3) RLSA designs with different section lengths (W_n). The relative permittivity values of S_1, S_2, S_3 are 1.03, 1.2 and 1.43, respectively. The permittivity values were kept constant for all the simulations. As it can be seen, equal section lengths are not optimal. By varying individual section lengths, it is possible to increase the bandwidth a lot at a very small expense of peak directivity. The section lengths shown in the second row, for example, leads to a 13.6% increase in directivity bandwidth over the design in the first row with equal section lengths, at the expense of only 0.1 dB drop in peak directivity.

TABLE III: Antenna performance for different values of section lengths.

Length of S_1 (W_1)	Length of S_2 (W_2)	Length of S_3 (W_3)	Peak directivity	3dB directivity bandwidth in the frequency range	3-dB directivity bandwidth	Aperture Efficiency
mm	mm	mm	dBi	GHz-GHz	(%)	(%)
66.7	66.7	66.7	27.9	9.2 - 11	17.8	36.6
80	**40**	**80**	**27.8**	**9.1 - 12.5**	**31.4**	**35.7**
100	40	60	27.6	9.2 - 12.6	31	34.1
100	60	40	27.3	9.3 - 12.7	30.9	31.8
80	60	60	27.3	9.2 - 12.5	30.4	31.8

B. Complete Design Example

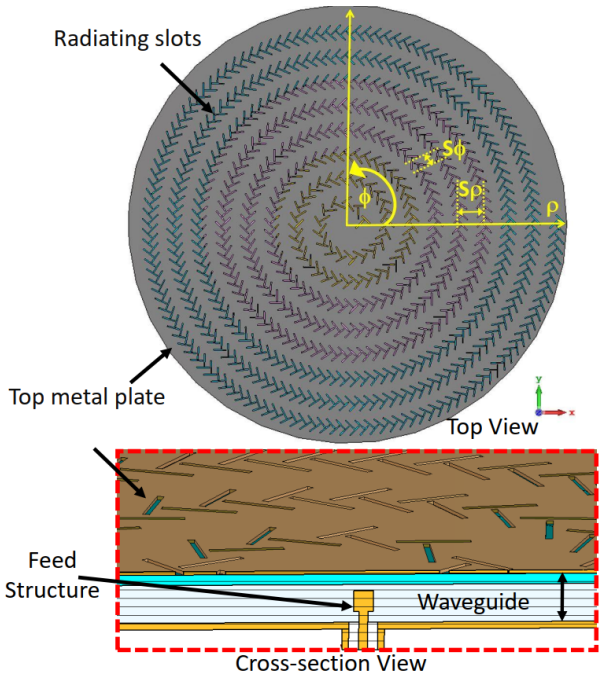

Fig. 6: Top view and cross-section view of the CP-RLSA antenna.

A multi-sectioned CP-RLSA antenna with 3 sections (S = 3), shown in Figure 6, was designed to operate at the center operating frequency of 11 GHz. Top plate is assumed to be 0.5 mm thick and it has 8 rings of radiating slots. The radiating slots are arrayed in a spiral pattern on the top plate. The radial distance S_ρ between two consecutive slot rings is 22.73 mm. The radius of the antenna aperture is 7.4$\lambda_\circ$ (200 mm).

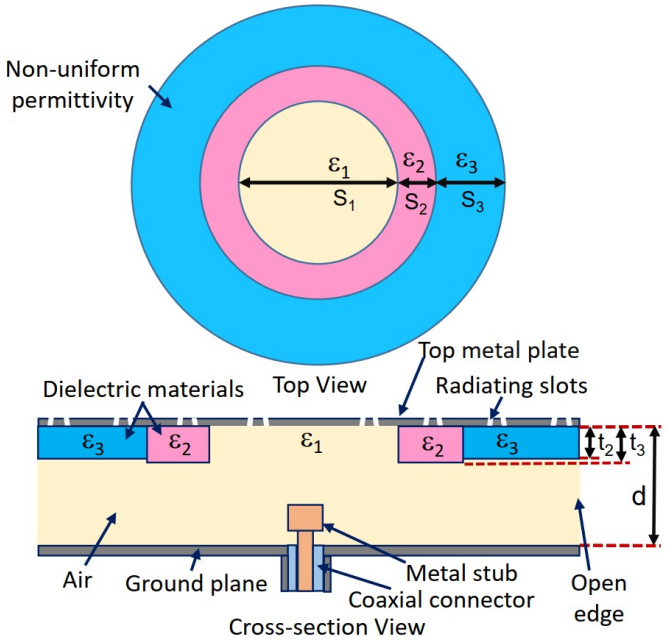

Fig. 7: Top view and cross-section view of the new waveguide.

The calculated effective dielectric constant values for the three sections are ϵ_1 = 1.03, ϵ_2 = 1.2 and ϵ_3 = 1.43. However, it is difficult to find commercially available dielectric materials with these dielectric constant values. So, the waveguide was filled with two layers of different materials. The lower part is filled with air as shown in Fig. 7 and the upper part is a commercially available dielectric layer with a thickness t.

The total waveguide height (d) was set to 7 mm, which is less than half of the guided wavelength in the most dense section S_3 at the expected highest operating frequency of 13 GHz ($\lambda_g/2$ = 9.65 mm). As the dielectric constant required for the first section (ϵ_1) is close to 1, the first section is totally filled with air. The thickness of the two dielectric layers (t_2 and t_3) were determined according to commercial availability. All design parameters of the non-uniform radial waveguide including sections lengths are given in Table IV.

TABLE IV: Waveguide design parameters.

Section	S_1	S_2	S_3
Material	Air	Roger 5880	Roger 3003
Dielectric constant	1	2.2	3
Loss tangent	0	0.0009	0.0019
Thickness	N/A	1.575	1.52
Effective dielectric constant	1	1.2	1.43
Length	80	40	80

The ground plate is also Aluminium and the end of the radial waveguide edge was left open, expecting that most of the energy in the outward travelling wave would radiate before reaching the end. A 50 Ω coaxial connector is inserted at the center of the ground plane to feed the waveguide. The coaxial pin of the connector extends into the air filled region of the waveguide and is terminated with an Aluminium disk-shaped metal stub as shown in Fig. 7. The metal stub has a thickness of 3 mm, diameter 2.8 mm, gap from ground plane 1.6 mm. The slot layout on the top surface was created using a custom-built Visual Basic interface in CST Microwave Studio. The antenna was simulated from 9 GHz to 13 GHz using the time-domain solver in CST Microwave Studio.

V. Results

A. Antenna Prototype

To validate the concept and predicted results, a prototype of the antenna was fabricated. The slot layout on the top aperture plate (Fig. 8(a)) was made out of a 0.5 mm thick stainless steel plate using laser cutting. To make the non-uniform radial waveguide, annular sections of dielectric materials Roger 5880 and Roger 3003 were cut to the right size and glued to the back of the top radiating plate. Around the edges of the top plate and ground plane 24 equally spaced holes were drilled with a diameter of 3 mm. Nylon screws were inserted through these holes, and together with 5.5 mm long spacers, they held the top radiating plate above the ground plane leaving the right gap in between.

B. Electric Near-field Distribution

Fig. 9 shows the electric field distribution near the aperture for five different frequencies. The electric field distributions have been extracted from the near-field data predicted from full-wave simulations. The plots represent the magnitude of the electric field component $|E_x|$. These field distributions were taken at a height of $1\lambda_\circ$ from the radiating plate on a plane parallel to the XY plane. As can be seen, at 9 GHz most of the radiation comes from the outer part (Section S_3) of the antenna. As the frequency increases the "hot region" shifts towards the center of the antenna. At 13 GHz, the center part (Section S_1) of the antenna radiates the best, as expected.

C. Input Matching

The predicted and measured input reflection coefficients ($|S_{11}|$) are shown in Fig. 10. These was measured using an Agilent PNA-X vector network analyzer. Fig. 10 demonstrates a good agreement between the predicted and measured $|S_{11}|$ with a measured 10dB return loss bandwidth extending from 9.15 GHz to beyond 13 GHz. It is found that $|S_{11}|$ remains below -10 dB over the entire 3-dB gain bandwidth (presented later).

D. Gain and Axial Ratio

Fig. 11 shows the predicted and measured broadside directivity, gain and aperture efficiency versus frequency. The gain was measured using the gain comparison method with WR-75 and WR-112 standard gain horns. The measured peak gain is 27.3 dBic and the measured 3dB gain bandwidth extends from 9.7 GHz to 12.8 GHz (27.6%). The dircetivity is 28.7 dBic and the measured 3dB directivity bandwidth is from 9.8 GHz to 12.7 GHz (25.8%). In general, the measured directivity

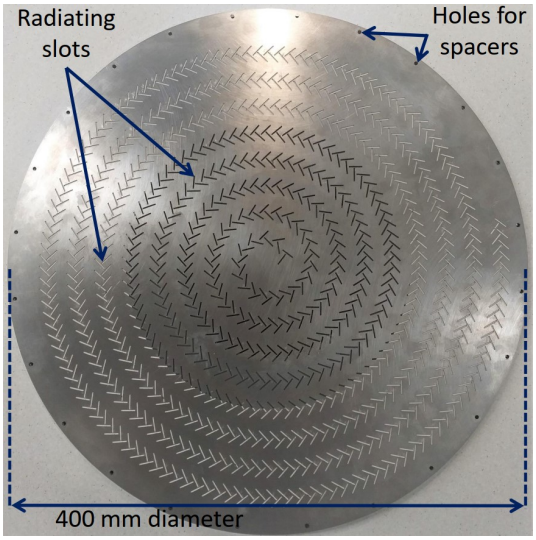

(a)

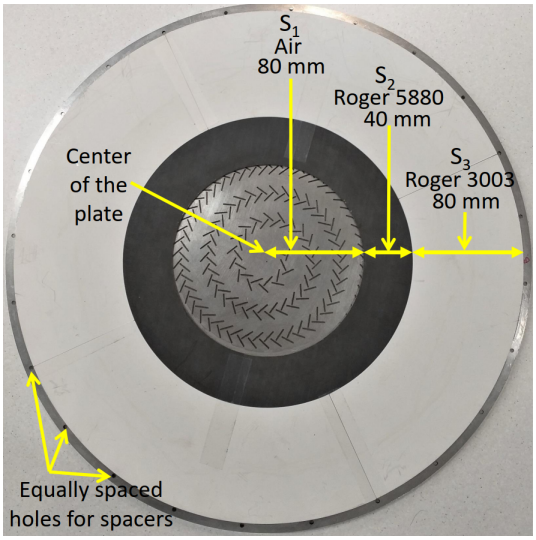

(b)

Fig. 8: Fabricated top part of the antenna (a) Front view of the top aperture plate, (b) Back view of the aperture plate, with glued annular dielectric sections when the ground plane is removed. In the middle, plate can be seen from the back as well because there is no dielectric in this section (S_1).

and gain curves closely follows the predicted ones, but with a slight upward shift in frequency due to fabrication tolerances.

In RLASs, like all other aperture antennas, the broadside directivity is proportional to the effective aperture, which depends on the uniformity in aperture phase distribution. The main parameter that controls the frequency of peak directivity in RLSAs is the radial distance between slot pairs. The primitive technique of gluing slotted metal sheet, which was deformed during laser cutting, on different rings of dielectrics is susceptible to create manufacturing errors.The technique has a high probability of leaving air pockets between the metal plate and the dielectrics and hence effectively reduces the electrical spacing between slots pairs, which would shift the results to higher frequencies. The antenna has an aperture efficiency of 28.3% at 10.4 GHz.

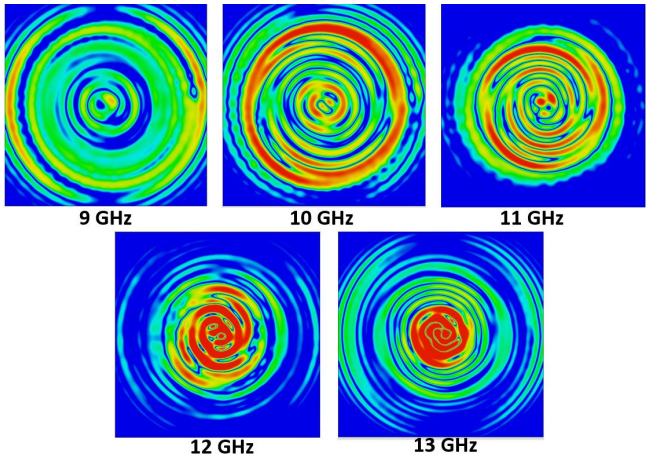

Fig. 9: The magnitude of the electric field component $|E_x|$ parallel to the XY plane at different frequencies.

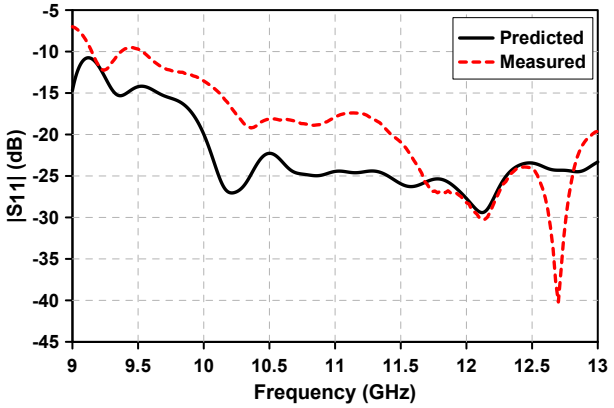

Fig. 10: Input reflection coefficient of the wideband CP-RLSA antenna.

Fig. 12 shows the broadside axial ratio of the antenna. It can be observed that the predicted and measured axial ratios are less than 3dB from 9.1 GHz and 9.5 GHz, respectively, to beyond 13 GHz, which confirms good circular polarization expected from the antenna over a wide frequency range.

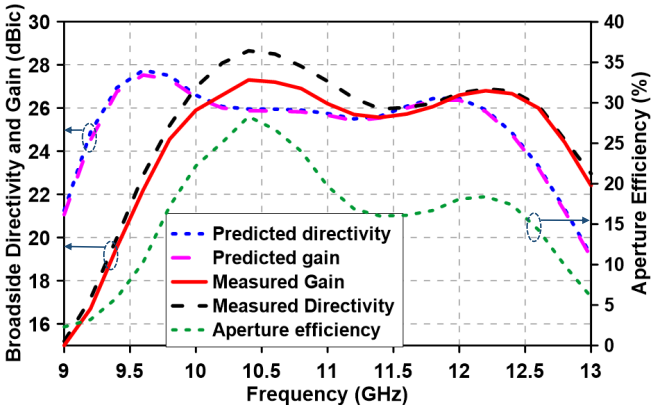

Fig. 11: Broadside directivity, gain and aperture efficiency of the wideband RLSA antenna.

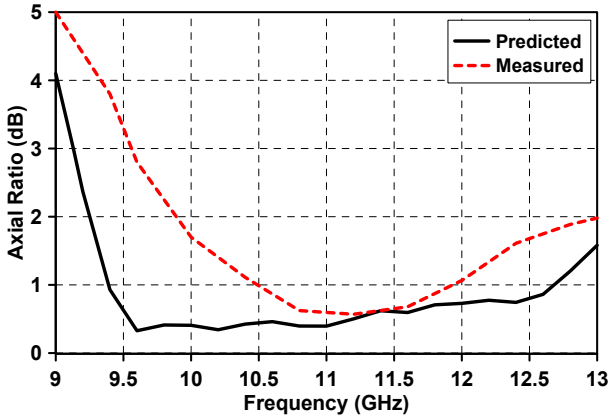

Fig. 12: Broadside axial ratio of the antenna.

E. Radiation pattern

The predicted and measured radiation patterns are shown in Fig. 13. The patterns are taken in the $\phi = 0°$ plane at four frequencies within the measured 3-dB gain bandwidth of the antenna. Fig. 14 shows the measured radiation patterns of the antenna in $\phi = 90°$ plane. Sidelobe levels (SLL) of about -7.4 dB is observed in the $\phi = 90°$ plane at 10 GHz; however, it remains below -10 dB at higher frequencies. Measured performance figures of the antenna at four frequencies are summarised in Table V. Phase errors are intrinsic in wideband designs. The overall performance of the antenna is found to be consistent with the predictions. This verifies the design methodology and confirms that a non-uniform radial waveguide made out of commercially available dielectric materials can be used to design wideband RLSA antenna.

TABLE V: Measured performance of the wideband RLSA at four frequencies.

Frequency (GHz)	10	11	12	12.6
θ_{3dB} ($\phi = 0°$) degrees	4.9	6.7	5.5	5.6
θ_{3dB} ($\phi = 90°$) degrees	4.8	6.7	4.9	6.2

VI. Discussion

In most antennas, bandwidth improvement is often accompanied by a decrease in the peak gain and aperture efficiency and the same was expected and noted in this research when a non-uniform radial waveguides were used to significantly increase the bandwidth of RLSA antennas. Therefore, it necessary to use figures of merit to compare different designs. The most relevant figures of merit for the high-gain wideband antennas are Gain Bandwidth Product (GBP) and Gain Bandwidth Product per unit Area (GBP/A). The latter is also proportional to the product of aperture efficiency and fractional bandwidth. The GBP is calculated by multiplying linear gain by the 3dB gain bandwidth (fractional or percentage) of the antenna. The GBP/A is the ratio of the GBP and the area of antenna, which is expressed in square wavelengths, covers all three aspects (gain, bandwidth and area) and in fact is related to Aperture Efficiency Bandwidth Product by a constant. In some previously published articles on extremely wideband resonant-cavity antennas, Directivity Bandwidth Product (DBP) and Directivity Bandwidth Product per unit Area (DBP/A) have been used as figures of merit [44].

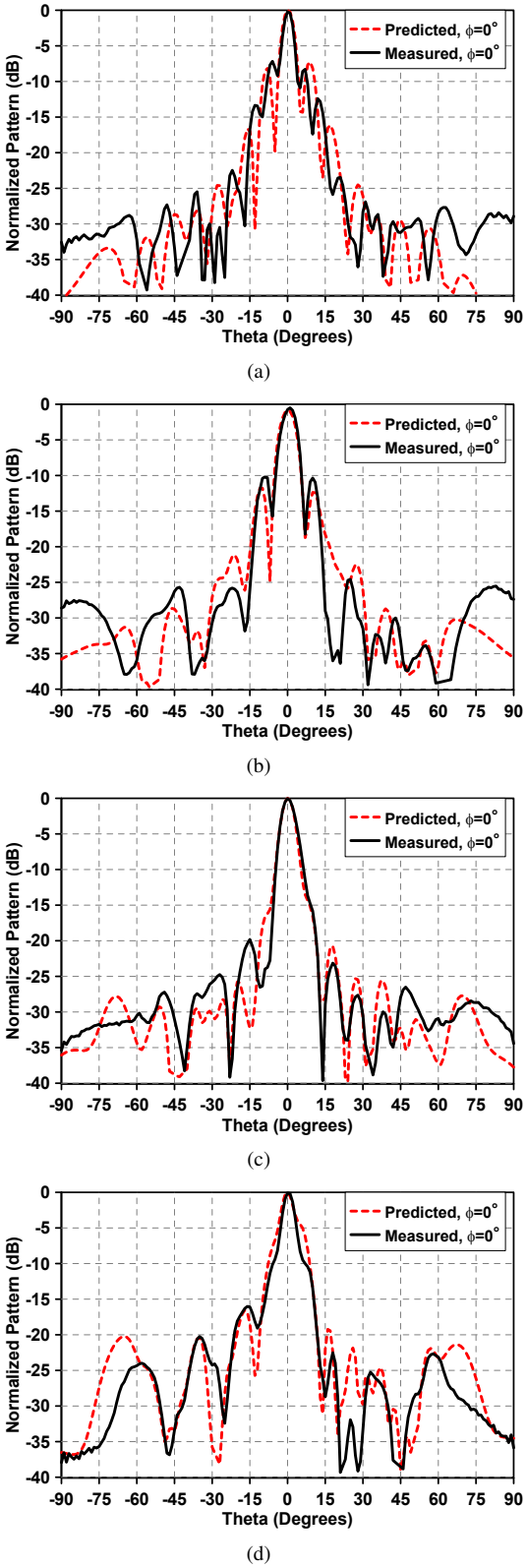

Fig. 13: Radiation patterns of the antenna on $\phi = 0°$ plane (a) 10 GHz (b) 11 GHz (c) 12 GHz (d) 12.6 GHz.

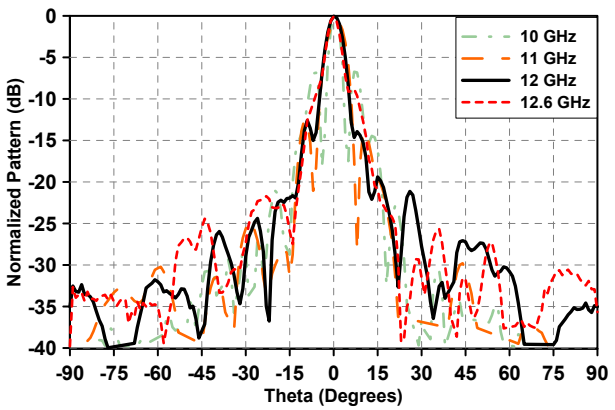

Fig. 14: Measured radiation patterns of the antenna on $\phi = 90^\circ$ plane.

We have included here a table comparing GBP and GBP/A of the new antenna with different RLSA antennas available in literature.

Table VI summarizes the electrical and physical characteristics of the new multi-section RLSA and several published conventional RLSAs. As it can be seen from the table that the new RLSA with non-uniform radial guide has much larger 3-dB gain bandwidth than previous RLSAs. It also has a very large GBP of 14,822 and a reasonably smaller footprint of $168.6\lambda_0^2$ at the center operating frequency. To the best of our knowledge, only few RLSA prototypes have demonstrated GBPs greater than 12,000 [26], [30], [35] but their area is more than twice of the new antenna. Yet the aperture efficiency of the new antenna is in the low range and hence it is important to consider GBP/A to see whether the trade-off between aperture efficiency and bandwidth has resulted in a positive dividend. The selection of dielectric material, lengths of slots and positions of the slots can be optimised in the future to improve other performance figures such as the aperture efficiency of the new antenna. Indeed yes, the new antenna has the highest GBP/A of 88 in addition to the widest measured 3-dB gain bandwidth. Further, its height is the second lowest in terms of wavelength at the centre frequency.

VII. Conclusion

With several design examples, it has been demonstrated that the gain bandwidth of an RLSA can be increased to previously impossible levels of 30-40% using the new method presented here that is by applying an appropriately designed non-uniform radial waveguide to feed the slot array. The predictions have been validated with experimental results of a prototype with 27.6% measured 3dB gain bandwidth and 27.3 dBic measured gain. Unprecedentedly high measured Gain Bandwidth Product per unit area of the prototype at 88 confirms excellent overall performance of the antenna in terms of gain, bandwidth and area.

In the case of CP-RLSAs good input matching and axial ratio are also achieved over an even larger bandwidth, leading to an overall bandwidth that is identical to the 3dB gain bandwidth. Large axial-ratio bandwidth is not a surprise because the phase orthogonality condition for CP (i.e. the separation between the two slots in a pair is quarter a guided wavelength) is automatically satisfied by each section when the condition for phase coherence for broadside radiation (S_ρ=$\lambda_{gn}(f)$) is satisfied at its best radiating frequency.

Moderate number of sections (3-4) are sufficient to achieve bandwidths in the order of 30% and they can be implemented in an RLSA with only minor increase in manufacturing complexity. Length of each section can be optimised, without increasing the total antenna area, to further optimise antenna performance. Readily available dielectric slabs with standard dielectric constants and thickness values can be used for implementation without compromising performance.

The maximum aperture efficiency of the new antenna in the operating band is around 30%. Such a reduced aperture efficiency is expected from Table II due to the segmentation of the aperture in such a way that each section radiates well in each sub-band. With a uniform TEM waveguide of single section, the same antenna would have aperture efficiencies in the range of 52.5%-57% (Table II) but the bandwidth would be much less, in the range of 6-8%. A previous RLSA prototype that was designed to have a more uniform aperture distribution has an aperture efficiency of 65% [6]. These figures indicate to what extent one has to compromise aperture efficiency when significantly increasing the bandwidth of an RLSA using a non-uniform TEM waveguide.

Radial non-uniformity of the effective dielectric constant of the waveguide can be continuous but for the sake of simple implementation only discrete changes have been considered in this paper. With this, RLSA antennas have become a low-profile antenna technology with excellent gains, bandwidths, radiation efficiencies, GBP/As and structural simplicity.

TABLE VI: Comparison of the measured characteristics of the new multi-section RLSA prototype with characteristics of previous conventional and wideband RLSA prototypes where measured gain bandwidth is available.

Ref	Gain	Aperture Effi-ciency	3dB gain band-width	Height	Gain BW prod-uct	Area	Gain BW prod-uct/ Area
Ref	dBi	%	%	λ_0	GBP	λ_0^2	GBP/ A
[35]	36	40.7	6.7	0.48	26,673.2	777.3	34.3
[30]	33.7	42.2	6.72	0.4	15,753	440.9	35.7
[26]	34.5	59	4.6	0.23	12,964.5	380.3	34
[14]	31	24.6	4.8	0.3	6,042.8	405.5	14.9
[45]	30.7	49.1	5.9	-	6,931.9	190	36.4
This work	27.3	28.3	27.6	0.29	14,822	168.6	88

Acknowledgment

This research has been supported by the Australian Research Council Discovery scheme and International Macquarie University Research Excellence Scholarship (iMQRES).

REFERENCES

[1] M. U. Afzal and K. P. Esselle, "Steering the beam of medium-to-high gain antennas using near-field phase transformation," *IEEE Trans. Antennas Propag.*, vol. 65, no. 4, pp. 1680–1690, April 2017.

[2] K. Singh, M. U. Afzal, M. Kovaleva, and K. P. Esselle, "Controlling the most significant grating lobes in two-dimensional beam-steering systems with phase-gradient metasurfaces," *IEEE Trans. Antennas Propag.*, pp. 1–1, 2019.

[3] A. A. Baba, R. M. Hashmi, K. P. Esselle, M. Attygalle, and D. Borg, "A millimeter-wave antenna system for wideband two-dimensional beam steering," *IEEE Trans. Antennas Propag.*, pp. 1–1, 2020.

[4] M. Ando, K. Sakurai, N. Goto, K. Arimura, and Y. Ito, "A radial line slot antenna for 12 GHz satellite TV reception," *IEEE Trans. Antennas Propag.*, vol. 33, no. 12, pp. 1347–1353, Dec 1985.

[5] M. Ando, K. Sakurai, and N. Goto, "Characteristics of a radial line slot antenna for 12 GHz band satellite TV reception," *IEEE Trans. Antennas Propag.*, vol. 34, no. 10, pp. 1269–1272, Oct 1986.

[6] M. Takahashi, J. I. Takada, M. Ando, and N. Goto, "A slot design for uniform aperture field distribution in single-layered radial line slot antennas," *IEEE Trans. Antennas Propag.*, vol. 39, no. 7, pp. 954–959, Jul 1991.

[7] Teddy Purnamirza, "Radial line slot array (rlsa) antennas," in *Telecommunication Systems*, Isiaka A. Alimi, Paulo P. Monteiro, and António L. Teixeira, Eds., chapter 10. IntechOpen, Rijeka, 2019.

[8] K. Kelly and F. Goebels, "Annular slot monopulse antenna arrays," *IEEE Trans. Antennas Propag.*, vol. 12, no. 4, pp. 391–403, Jul 1964.

[9] M. Ando, T. Numata, J. I. Takada, and N. Goto, "A linearly polarized radial line slot antenna," *IEEE Trans. Antennas Propag.*, vol. 36, no. 12, pp. 1675–1680, Dec 1988.

[10] M. Ando, "New DBS receiver antennas," in *1993 23rd European Microwave Conference*, Sept 1993, pp. 84–92.

[11] P. W. Davis and M. E. Bialkowski, "Experimental investigations into a linearly polarized radial slot antenna for DBS TV in Australia," *IEEE Trans. Antennas Propag.*, vol. 45, no. 7, pp. 1123–1129, Jul 1997.

[12] J. Takada, M. Ando, and N. Goto, "A reflection cancelling slot set in a linearly polarized radial line slot antenna," *IEEE Trans. Antennas Propag.*, vol. 40, no. 4, pp. 433–438, Apr 1992.

[13] Paul William Davis, "A linearly polarised radial line slot array antenna for direct broadcast satellite services," PhD dissertation, University of Queensland, Australia, 2000.

[14] P. W. Davis and M. E. Bialkowski, "Linearly polarized radial-line slot-array antennas with improved return-loss performance," *IEEE Antennas and Propagation Magazine*, vol. 41, no. 1, pp. 52–61, Feb 1999.

[15] M. E. Bialkowski and P. W. Davis, "Analysis of a circular patch antenna radiating in a parallel-plate radial guide," *IEEE Trans. Antennas Propag.*, vol. 50, no. 2, pp. 180–187, Feb 2002.

[16] N. Y. Koli, M. U. Afzal, K. P. Esselle, L. Matekovits, and Z. Islam, "Investigating small aperture radial line slot array antennas for medium gain communication links," in *2019 International Conference on Electromagnetics in Advanced Applications (ICEAA)*, 2019, pp. 0613–0616.

[17] N. Y. Koli, M. U. Afzal, K. P. Esselle, and M. Zahidul Islam, "Analyzing the coupling from radiating slots in a double-layered radial line slot array antenna," in *2019 IEEE International Symposium on Antennas and Propagation and USNC-URSI Radio Science Meeting*, 2019, pp. 1427–1428.

[18] S. I. Zakwoi, T. A. Rahman, I. Maina, and O. Elijah, "Design of Ka band downlink radial line slot array antenna for direct broadcast satellite services," in *2014 IEEE Asia-Pacific Conference on Applied Electromagnetics (APACE)*, Dec 2014, pp. 159–162.

[19] A. Mazzinghi, M. Albani, and A. Freni, "Double-spiral linearly polarized RLSA," *IEEE Trans. Antennas Propag.*, vol. 62, no. 9, pp. 4900–4903, Sept 2014.

[20] M. N. Y. Koli, M. U. Afzal, K. P. Esselle, and R. M. Hashmi, "An all-metal high-gain radial-line slot-array antenna for low-cost satellite communication systems," *IEEE Access*, vol. 8, pp. 139422–139432, 2020.

[21] J. Suryana and D. B. Kusuma, "Design and implementation of RLSA antenna for mobile DBS application in Ku-band downlink direction," in *2015 International Conference on Electrical Engineering and Informatics (ICEEI)*, Aug 2015, pp. 341–345.

[22] María Vera-Isasa, M. Sierra-Castaner, and Manuel Sierra Perez, "Design of circular polarized radial line slot antennas.," *I. J. Wireless and Optical Commun.*, vol. 1, pp. 179–189, 12 2003.

[23] M. Takahashi, M. Ando, N. Goto, Y. Numano, M. Suzuki, Y. Okazaki, and T. Yoshimoto, "Dual circularly polarized radial line slot antennas," *IEEE Trans. Antennas Propag.*, vol. 43, no. 8, pp. 874–876, Aug 1995.

[24] M. Sierra-Castaner, M. Sierra-Perez, M. Vera-Isasa, and J. L. Fernandez-Jambrina, "Low-cost monopulse radial line slot antenna," *IEEE Trans. Antennas Propag.*, vol. 51, no. 2, pp. 256–263, Feb 2003.

[25] TS Lim and KG Tan, "The development of radial line slot array antenna for direct broadcast satellite reception," *International journal of electronics*, vol. 94, no. 3, pp. 251–261, 2007.

[26] M. Albani, A. Mazzinghi, and A. Freni, "Automatic design of CP-RLSA antennas," *IEEE Trans. Antennas Propag.*, vol. 60, no. 12, pp. 5538–5547, Dec 2012.

[27] J. M. Fernandez Gonzalez, P. Padilla, G. Exposito-Dominguez, and M. Sierra-Castaner, "Lightweight portable planar slot array antenna for satellite communications in X-Band," *IEEE Antennas Wireless Propag. Lett.*, vol. 10, pp. 1409–1412, 2011.

[28] C. W. Yuan, S. R. Peng, T. Shu, Z. Q. Li, and H. Wang, "Designs and experiments of a novel radial line slot antenna for high-power microwave application," *IEEE Trans. Antennas Propag.*, vol. 61, no. 10, pp. 4940–4946, Oct 2013.

[29] N. Y. Koli, M. U. Afzal, K. P. Esselle, R. M. Hashmi, and M. Z. Islam, "A low-profile and efficient front-end antenna for point-to-point wireless communication links," in *2020 14th European Conference on Antennas and Propagation (EuCAP)*, 2020, pp. 1–4.

[30] T. Yamamoto, M. Takahashi, M. Ando, and N. Goto, "Measured performances of a wide band radial line slot antenna," in *Proceedings of IEEE Antennas and Propagation Society International Symposium and URSI National Radio Science Meeting*, June 1994, vol. 3, pp. 2204–2207 vol.3.

[31] L. Yuan, M. Su, Y. Liu, S. Li, and X. Miao, "A linearly polarized radial line dielectric resonator antenna array," in *2015 International Symposium on Antennas and Propagation (ISAP)*, Nov 2015, pp. 1–4.

[32] S. Peng, C. W. Yuan, T. Shu, J. Ju, and Q. Zhang, "Design of a concentric array radial line slot antenna for high-power microwave application," *IEEE Transactions on Plasma Sci.*, vol. 43, no. 10, pp. 3527–3529, Oct 2015.

[33] S. Peng, C. Yuan, T. Shu, and X. Zhao, "Linearly polarised radial line slot antenna for high-power microwave application," *IET Microwaves, Antennas Propagation*, vol. 11, no. 5, pp. 680–684, 2017.

[34] Serguei Zagriatski and Marek E. Bialkowski, *Low-Cost Circularly Polarized Radial Line Slot Array Antenna for IEEE 802.11 B/G WLAN Applications*, pp. 197–210, Springer US, Boston, MA, 2005.

[35] T. Yamamoto, S. Hagiwara, J. Takada, M. Takahashi, M. Ando, and N. Goto, "A wide band radial line slot antenna," in *proceesings of ISAP '92, Sapporo, Japan*, 1992, pp. 29–32.

[36] T. Yamamoto, M. Ando, and N. Goto, "A concentric array wide-band radial line slot antenna with matching terminating slots," in *IEEE Antennas and Propagation Society International Symposium. 1995 Digest*, June 1995, vol. 4, pp. 1990–1993 vol.4.

[37] Tetsuya Yamamoto, Migaku Takahashi, Makoto Ando, and Naohisa Goto, "Enhancement of band-edge gain in radial line slot antennas using the power divider–a wide-band radial line slot antenna–," *IEICE Transactions on Communications*, vol. 78, pp. 398–406, 1995.

[38] Valero-Nogueira, Herranz, Antonino, and Cabedo-Fabres, "Linearly polarized radial line slot array antenna with wideband return loss performance using a multisleeve coaxial transition," *IEEE Antennas Wireless Propag. Lett.*, vol. 3, pp. 348–350, 2004.

[39] Ibrahim Maina, Tharek Abd Rahman, Mohsen Khalily, and Solomon Iliya, "Multilayered cavity material radial line slot array antenna with improved bandwidth for 5g communication application," *Modern Applied Science*, vol. 10, pp. 134 – 141, 06 2016.

[40] R Kamaruddin, Imran Ibrahim, M Rahim, Zulkifli Zakaria, Noor Azwan Shairi, and T Rahman, "Radial line slot array (rlsa) antenna design at 28 ghz using air gap cavity structure," *Journal of Telecommunication, Electronic and Computer Engineering*, vol. 9, 10 2017.

[41] I. M. Ibrahim, T. Purnamirza, T. A. Rahman, and M. I. Sabran, "Radial line slot array antenna development in malaysia," in *2013 7th European Conference on Antennas and Propagation (EuCAP)*, 2013, pp. 174–178.

[42] Ibrahim Maina, Tharek Abd Rahman, and Mohsen Khalily, "Bandwidth enhanced and sidelobes level reduced radial line slot array antenna at 28 GHz for 5G next generation mobile communication," *ARPN Journal of Engineering and Applied Sciences*, vol. 10, pp. 5752–5757, 2015.

[43] I. M. Ibrahim, T. A. Rahman, M. I. Sabran, and M. F. Jamlos, "Bandwidth enhancement through slot design on rlsa performance," in *2014 IEEE REGION 10 SYMPOSIUM*, 2014, pp. 228–231.

[44] A. A. Baba, R. M. Hashmi, and K. P. Esselle, "Achieving a large gain-bandwidth product from a compact antenna," *IEEE Trans. Antennas Propag.*, vol. 65, no. 7, pp. 3437–3446, 2017.
[45] J. I. Herranz, A. Valero-Nogueira, F. Vico, and V. M. Rodrigo, "Optimization of beam-tilted linearly polarized radial-line slot-array antennas," *IEEE Antennas Wireless Propag. Lett.*, vol. 9, pp. 1165–1168, 2010.

Mst Nishat Yasmin Koli (S'17) received the B.S. degree in electronics and telecommunication engineering from Rajshahi University of Engineering and Technology (RUET), Rajshahi, Bangladesh in 2015 and Master by Research (MRes) degree in Electronics Engineering from Macquarie University, Sydney, Australia, in 2017. She is currently pursuing Ph.D. degree with the Centre for Collaboration in Electromagnetic and Antenna Engineering (CELANE), Macquarie University, Sydney, NSW, Australia.

From 2015 to 2016, she was a lecturer in electrical and electronics engineering department, European University, Dhaka, Bangladesh. Her research interests include antenna array, high-gain planar metasurface based antennas, radial-line slot array antennas, beam steering metasurfaces, antennas for radio astronomy and satellite communication, and microwave and millimetre-wave antennas. She received several prestigious awards, including the International Research Training Program Scholarship (iRTP) for the MRes and International Macquarie University Research Excellence Scholarship (iMQRES) for her Ph.D. degree.

Muhamamd U. Afzal (S'13–M'16) received the B.S. degree in electronics engineering (hons.) and Master's degree in Computational Science and Engineering from National University of Sciences and Technology (NUST), Islamabad, Pakistan, in 2005 and 2011, respectively. He completed his PhD in electronics engineering from Macquarie University in 2016.

From 2010 to 2012, he was a lab engineer at Samar Mubarakmand Research Institute of Microwave and Millimeterwave Studies (SMRIMMS), Islamabad, Pakistan. From 2012 to 2013, he was a lecturer in the electrical engineering department, NUST, Islamabad, Pakistan. He is now a research associate in Electromagnetic and Antenna Engineering at the University of Technology Sydney. His research interests include electromagnetic band gap or Fabry-Perot resonator antennas, high-gain planar metasurface based antennas, radial-line slot antennas, phased arrays, free-standing phase-shifting structures or metasurfaces, frequency selective surfaces, near-field phase transformation, and far-field pattern synthesis using near-field phase transformation.

Mr. Muhammad received NUST merit base scholarship during undergraduate studies and International Macquarie Research Excellence Scholarship (iMQRES) for PhD studies.

Professor Karu Esselle IEEE 'M (1992), SM (1996), F (2016), is the Distinguished Professor in Electromagnetic and Antenna Engineering at the University of Technology Sydney and a Visiting Professor of Macquarie University, Sydney. According to a Special Report on Research published by The Australian national newspaper in 2019, he is the National Research Field Leader in Australia in Microelectronics in Engineering Discipline as well as in the Electromagnetism field in the Disciplines of Physics and Mathematics.

Karu received BSc degree in electronic and telecommunication engineering with First Class Honours from the University of Moratuwa, Sri Lanka, and MASc and PhD degrees with near-perfect GPA in electrical engineering from the University of Ottawa, Canada. Previously he was Director of WiMed Research Centre and Associate Dean – Higher Degree Research (HDR) of the Division of Information and Communication Sciences and directed the Centre for Collaboration in Electromagnetic and Antenna Engineering at Macquarie University. He has also served as a member of the Dean's Advisory Council and the Division Executive and as the Head of the Department several times. Karu is a Fellow of IEEE, the Royal Society of New South Wales and Engineers Australia.

Since 2018, Karu has been chairing the prestigious Distinguished Lecturer Program Committee of the IEEE Antennas and Propagation (AP) Society – the premier global learned society dedicated for antennas and propagation - which has close to 10,000 members worldwide. After two stages in the selection process, Karu was also selected by this Society as one of two candidates in the ballot for 2019 President of the Society. Only three people from Asia or Pacific apparently have received this honour in the 68-year history of this Society. Karu is also one of the three Distinguished Lecturers (DL) selected by the Society in 2016. He is the only Australian to chair the AP DL Program ever, the only Australian AP DL in almost two decades, and second Australian AP DL ever (after UTS Distinguished Visiting Professor Trevor Bird). He has been continuously serving the IEEE AP Society Administrative Committee in several elected or ex-officio positions since 2015. Karu is also the Chair of the Board of management of Australian Antenna Measurement Facility, and was the elected Chair of both IEEE New South Wales (NSW), and IEEE NSW AP/MTT Chapter, in 2016 and 2017.

Karu has authored approximately 600 research publications and his papers have been cited over 10,000 times. In 2019 his publications received 1,200 citations. He is the first Australian antenna researcher ever to reach Google Scholar h-index of 30 and his citation indices have been among the top Australian antenna researchers for a long time (at present: i10 is 180 and h-index is 49). Since 2002, his research team has been involved with research grants, contracts and PhD scholarships worth about 20 million dollars, including 15 Australian Research Council grants, without counting the 245 million-dollar SmartSat Corporative Research Centre, which started in 2019. His research has been supported by many national and international organisations including Australian Research Council, Intel, US Air Force, Cisco Systems, Hewlett-Packard, Australian Department of Defence, Australian Department of industry, and German and Indian governments.

Karu's awards include one of the two finalists for 2020 Australian Eureka Prize for Outstanding Mentor of Young Researchers, 2019 Motohisa Kanda Award (from IEEE USA) for the most cited paper in IEEE Transactions on EMC in the past five years, 2019 Macquarie University Research Excellence Award for Innovative Technologies, 2019 ARC Discovery International Award, 2017 Excellence in Research Award from the Faculty of Science and Engineering, 2017 Engineering Excellence Award for Best Innovation, 2017 Highly Commended Research Excellence Award from Macquarie University, 2017 Certificate of Recognition from IEEE Region 10, 2016 and 2012 Engineering Excellence Awards for Best Published Paper from IESL NSW Chapter, 2011 Outstanding Branch Counsellor Award from IEEE headquarters (USA), 2009 Vice Chancellor's Award for Excellence in Higher Degree Research Supervision and 2004 Innovation Award for best invention disclosure. His mentees have been awarded many fellowships, awards and prizes for their research achievements. Fifty international experts who examined the theses of his PhD graduates ranked them in the top 5% or 10%.

Karu has provided expert assistance to more than a dozen companies including Intel, Hewlett Packard Laboratory (USA), Cisco Systems (USA), Audacy (USA), Cochlear, Optus, ResMed and Katherine-Werke (Germany). His team designed the high-gain antenna system for the world's first entirely Ka-band CubeSat made by Audacy, USA and launched to space by SpaceX in December 2018. This is believed to be the first Australian-designed high-gain antenna system launched to space, since CSIRO-designed antennas in Australia's own FedSat launched in 2002.

Karu is in the College of Expert Reviewers of the European Science Foundation (2019-22) and he has been invited to serve as an international

expert/research grant assessor by several other research funding bodies as well, including the European Research Council and funding agencies in Norway, Belgium, the Netherlands, Canada, Finland, Hong-Kong, Georgia, South Africa and Chile. He has been invited by Vice-Chancellors of Australian and overseas universities to assess applications for promotion to professorial levels. He has also been invited to assess grant applications submitted to Australia's most prestigious schemes such as Australian Federation Fellowships and Australian Laureate Fellowships. In addition to the large number of invited conference speeches he has given, he has been an invited plenary/extended/keynote speaker of several IEEE and other conferences and workshops including EuCAP 2020 Copenhagen, Denmark; URSI'19 Seville, Spain; and 23rd ICECOM 2019, Dubrovnik, Croatia.

He is an Associate Editor of IEEE Transactions on Antennas Propagation, IEEE Antennas and Propagation Magazine and IEEE Access. He is a Track Chair pf IEEE AP-S 2020 Montreal, Technical Program Committee Co-Chair of ISAP 2015, APMC 2011 and TENCON 2013 and the Publicity Chair of ICEAA/IEEE APWC 2016, IWAT 2014 and APMC 2000. His research activities are posted in the web at http://web.science.mq.edu.au/ esselle/ and https://www.uts.edu.au/staff/karu.esselle .